

Effect of pion external distortion on low-energy pion double charge exchange

M. Kh. Khankhasayev

Laboratory of Theoretical Physics, Joint Institute for Nuclear Research, Dubna 141980, Russia

H. Sarafian

Department of Physics, Pennsylvania State University, York, Pennsylvania 17403

Mikkel B. Johnson

Los Alamos National Laboratory, Los Alamos, New Mexico 87545

Zh. B. Kurmanov

Institute of Nuclear Physics, National Nuclear Center, Alma-Ata 480082, Republic of Kazakhstan

(Received 3 May 1993)

We simplify a treatment of pion distortions using a separable expansion of optical potential in momentum space. We use this method to gain insight into the role of distortions in isoelastic pion charge-exchange scattering within the framework of the isospin-invariant optical model. The method provides an analytic procedure for calculating external distortions of single- and double-charge-exchange scattering. This allows us to analyze separately the role of on- and off-shell pions in distortions for each partial wave. Results for sequential scattering at 50 MeV for the reaction $^{14}\text{C}(\pi^+, \pi^-)^{14}\text{O}$ are presented. It is shown that the external distortions give a small enhancement in forward directions and reduce the differential cross sections at large angles.

PACS number(s): 25.80.Gn

I. INTRODUCTION

In recent years, a pion-nucleus double-charge-exchange (DCX) scattering to the double-isobaric analog state (DIAS) has been studied systematically at low energies ($T = 50$ MeV) [1–4] and has attracted considerable interest. This interest has arisen because in this case the rather weak π - N interaction allows a relatively deep penetration of a pion into a nucleus. This is in contrast to the situation in the resonance region, where pions are scattered mostly by the nucleus surface. Thus, low-energy pions provide a useful means to probe the nuclear interior. Moreover, because the pion changes its charge by two units, it must interact with at least two nucleons. Hence the increased penetrability of low-energy pions on the one hand and the two-body character of DCX on the other provide an excellent opportunity for extracting information on interesting topics such as dynamical short-range correlations of nucleons and isospin triplet coupling of nucleon pairs.

Globally, there are two striking characteristics associated with low-energy pion DCX to the DIAS. The first one is that the magnitudes of the measured cross sections are comparable to those of the resonance region. The second one is that the differential cross sections are forward peaked. There are a number of microscopic mechanisms which have been proposed in attempts to describe these features [4–16].

Most the theoretical efforts have been devoted to clarifying the role of conventional sequential scattering (SEQ-

π), which occurs when two pion single-charge-exchange scatterings take place successively on different nucleons [5–9]. One can summarize the results for SEQ- π , calculated in the plane-wave approximation, as follows. (a) The calculated differential cross sections qualitatively reproduce the angular distributions, but they underestimate the latter by more than a factor of 2; only in Ref. [7] has a quantitative description of DCX scattering data in the plane-wave approximation been obtained. (b) The plane-wave results for SEQ- π are very sensitive to the nuclear structure [5,6], to short-range correlation effects [5], to the range of pion-nucleon form factor [5,8], and to uncertainties in the Δ - N interaction (especially within the framework of the Δ -hole model [6]).

In a number of studies, it has been shown that there can be a significant contribution to DCX from nonconventional mechanisms such as meson-exchange currents (MEC) [12,13] and absorption-channel effects [10,11]. According to these reports, each of the individual “exotic” mechanisms interferes constructively with the SEQ- π process at low energies and reproduces the experimental DCX angular distributions almost perfectly. It should be stressed, however, that these results have been obtained in the plane-wave approximation and that the significance of the agreement is therefore unclear at the present time.

The effect of pion distortions for the SEQ- π mechanism has been studied in several papers [4,6–9]. Distortions arise both from multiple scattering of the in- and out-going charged pions (external distortion) and from

multiple scattering of the intermediate neutral pion (internal distortion). In the Bleszynsky-Glauber paper [7], it was argued that distortions are of no importance at low energies and can be neglected. In contrast to this, a strong pion-distortion effect (external + internal) was found in Refs. [6,4]. In these two papers, it was found that by turning on the pion distortion the plane-wave results were magnified by a factor of 2. Additionally, it was reported that the main effect arose from the distortion of the intermediate pion; turning of this distortion strongly decreased the cross section. On the other hand, in Ref. [9], it was found that removing the internal distortion would generally increase the calculated cross sections. The effect of external distortions was studied recently within the framework of the distorted-wave impulse approximation (DWIA) in Ref. [8], where the authors claimed that the distortion of the external pion considerably changes the cross section, raising it above the plane-wave result at forward angles and lowering it below this result at large angles.

From the above discussion, one can see that the situation with pion distortions in sequential scattering is controversial and that there is room for further study. Two considerations have led us to develop a new analytic approach for handling the external distortions. The first is the observation that the standard DWIA calculation is a rather complicated procedure. The second is our belief that, to understand the physics of double charge exchange, one needs a detailed understanding of the interplay among distortions, the reaction mechanism, and the cross section. Although approximate, our approach is intended to provide a quantitative and more transparent means for gaining insight into the relationship between the DCX reaction and the nature of the pion optical potential. Having such a treatment of the external distortion is also advantageous because the same formulation as we have applied here to sequential pion scattering may also be applied to treat the nonconventional, exotic mechanisms, where only external distortions of the pions are required.

To calculate the external distortions, we have developed a procedure based on approximating our assumed optical potential by a separable interaction. This makes it possible to represent the distorted-wave (DW) DCX amplitude as a product of the plane-wave (PW) amplitude and a distortion factor in any given partial-wave channel. This distortion factor is calculated in terms of pion-nucleus form factors, which we obtain using the Bateman separable approximation method [23]. According to the Bateman method, these form factors determine the off-energy-shell behavior of the elastic scattering amplitude.

This paper is organized as follows. In Sec. II, we present the general formalism within the framework of the isospin-invariant model: the two-potential formula for the DCX amplitude is derived and an expression for the DW amplitude in the separable approximation is obtained. Section III is devoted to the calculation of the π -nucleus form factors. In Sec. IV, we present results and conclusions. In the Appendix the details of constructing the isotensor potential U_2^{SEQ} are given.

II. FORMALISM

A. Isospin-invariant optical model

As described in the Introduction, the purpose of this paper is to characterize the contribution of the pion external distortion to pion double charge exchange. We have considered this problem within the context of an isospin-invariant optical model, in which the pion-nucleus isoelastic scattering (single and double charge exchange to isobaric analog states, as well as elastic scattering) is related to the strong interaction through isospin symmetry [14–16]. If we assume that the isospin breaking effects can be ignored, the optical potential has the form

$$\hat{U} = U_0 + U_1(\boldsymbol{\phi} \cdot \mathbf{T}) + U_2(\boldsymbol{\phi} \cdot \mathbf{T})^2, \quad (1)$$

where $\boldsymbol{\phi}$ (\mathbf{T}) is the pion (nucleus) isospin operator [14]. We assume that the isoscalar (U_0) and isovector (U_1) potentials are known and are fitted to the elastic and single-charge-exchange data [14–16].

In this theory, the π -nucleus scattering T matrix

$$\hat{T} = \mathcal{T}_0 + \mathcal{T}_1(\boldsymbol{\phi} \cdot \mathbf{T}) + \mathcal{T}_2(\boldsymbol{\phi} \cdot \mathbf{T})^2 \quad (2)$$

has an isospin structure identical to that of U . In terms of the T matrix, the DCX amplitude to the DIAS is given by

$$\langle \pi^-; \text{DIAS} | \hat{T} | \pi^+; \text{g.s.} \rangle = \sqrt{T_0(2T_0 - 1)} \mathcal{T}_2, \quad (3)$$

where T_0 is the z component of the nuclear isospin $T_0 = (N - Z)/2$, $|\text{g.s.}\rangle = |T_0, -T_0\rangle$ and $|\text{DIAS}\rangle = |T_0, -T_0 + 2\rangle$.

As we will show in the next section within the framework of the two-potential formalism, the amplitude in Eq. (3) consists of two pieces. The first arises from the iterations of U_0 and U_1 ; that occurs when the equations of motion are solved and describes DCX mediated by a scattered pion and a nucleus excited to the isobaric analog state. This piece, called the analog route (AR), is quite large in many cases and is tightly constrained by both empirical and theoretical considerations.

The second contribution to DCX comes from all processes except the sequential scattering through the isobaric analog intermediate state. This includes an excitation of the nucleus through intermediate nonanalog states as well as excitation of the meson and baryon fields themselves. These are represented by the isotensor term (U_2) in the optical potential. In this paper, we will take for U_2 a piece of the complete isotensor interaction that is known to be particularly important, namely, U_2^{NAR} . We construct this “nonanalog-route” (NAR) contribution theoretically from the SEQ mechanism of Ref. [5] (see the Appendix). First, an isotensor potential U_2^{SEQ} is formed from a model sequential scattering [5] built up from nonanalog excitations of the intermediate nucleus, including the effects of short-range nucleon-nucleon correlations, the intermediate ρ meson, and finite-range meson-nucleon form factors. Second, the contribution ΔU^{AR} of U_2^{SEQ} arising from the DCX transitions through the analog intermediate states is subtracted out,

$$U_2 = U_2^{\text{NAR}} \equiv U_2^{\text{SEQ}} - \Delta U_2^{\text{AR}}. \quad (4)$$

This subtraction avoids a double counting with the AR contribution discussed above. Later, in Sec. IV, we compare ΔU_2^{AR} with the analog-route calculations obtained from Ref. [16] to examine the differences reflecting the importance of medium modifications (second-order effects) in U_1 .

B. Two-potential formalism

Let us represent the optical potential Eq. (1) in the form

$$\hat{U} = \hat{V} + \hat{R}, \quad (5)$$

where

$$\hat{V} = U_0 + U_1(\boldsymbol{\phi} \cdot \mathbf{T}), \quad (6)$$

$$\hat{R} = U_2(\boldsymbol{\phi} \cdot \mathbf{T})^2. \quad (7)$$

Since $U_2 \ll U_1 \ll U_0$ [16], the isotensor term U_2 could be considered as a perturbation to the elastic and SCX channels. Therefore, within the framework of the two-potential formalism [17], we obtain the following expression for the total scattering matrix:

$$\mathcal{T} = T_V + \Omega_V^{(-)+} [\hat{R} + \hat{R} \mathcal{G}_P^{(+)} \hat{R}] \Omega_V^{(+)}, \quad (8)$$

where $\mathcal{G}_P^{(+)}$ is a full Green function,

$$\mathcal{G}_P^{(+)} = [E - \mathcal{H} \pm i\delta]^{-1}, \quad (9)$$

for the Hamiltonian

$$\mathcal{H} = K_\pi + H_A + \hat{U}. \quad (10)$$

Here T_V is the scattering matrix and $\Omega_V^{(\pm)}$ is a Möller operator for the Hamiltonian

$$\mathcal{H}_V = K_\pi + H_A + \hat{V}, \quad (11)$$

where K_π is a pion kinetic-energy operator, H_A is the

nuclear Hamiltonian, and V is given by Eq. (6). The Möller operator is expressed in terms of the T_V matrix as

$$\Omega_V^{(\pm)} = 1 + \hat{P} G^{(\pm)} T_V^{(\pm)}, \quad (12)$$

where $G^{(\pm)}$ is a free Green function,

$$G^{(\pm)}(E) = (E - K_\pi - H_A \pm i\delta)^{-1}, \quad (13)$$

and $\hat{P} = |0\rangle\langle 0|$ is a projection operator into the nuclear isobar analog states (ground states).

For DCX scattering to DIAS we get

$$\langle \pi^-; \text{DIAS} | \mathcal{T} | \pi^+; \text{g.s.} \rangle = T_V^{\text{AR}} + \sqrt{T_0(2T_0 - 1)} \mathcal{T}_2^{\text{DWBA}}. \quad (14)$$

Here T_V^{AR} is the contribution to DCX through the AR transitions (at least two actions of the isovector potential). The second term in Eq. (14) is the distorted-wave Born approximation (DWBA) for the isotensor amplitude,

$$\mathcal{T}_2^{\text{DWBA}} = \langle \psi_{\mathbf{k}_i}^{(-)}(\pi^-; \text{DIAS} | U_2 | \psi_{\mathbf{k}_i}^{(+)}(\pi^+; \text{g.s.}) \rangle, \quad (15)$$

where

$$\psi_{\mathbf{k}}^{(\pm)} = \Omega_V^{(\pm)} |\mathbf{k}\rangle. \quad (16)$$

From Eqs. (14) and (16), it follows that the procedure of taking into account the pion distortion consists of (a) taking the distorted-wave matrix element of U_2 , and (b) adding the term T^{AR} , which describes the contribution to DCX through the AR transitions. This is to be contrasted to the expression for the DCX cross section in the plane-wave Born approximation of U , which would give

$$\mathcal{T}_2^{\text{PWBA}} \equiv \langle \pi^-; \text{DIAS} | U_2 | \pi^+; \text{g.s.} \rangle.$$

C. Distortion factors

Introducing a complete set of intermediate pion-nucleus plane-wave states, one can rewrite Eq. (15) in the form

$$\mathcal{T}_2^{\text{DWBA}}(E) = \sum_{\bar{q}_1, \bar{q}_2} D_{\pi^-, \text{DIAS}}^{(-)}(\mathbf{k}_f, \mathbf{q}_1; E) \langle \pi^-, \mathbf{q}_1; \text{DIAS} | \mathcal{T}_2^{\text{PWBA}}(E) | \pi^+, \mathbf{q}_2; \text{g.s.} \rangle D_{\pi^+, \text{g.s.}}^{(+)}(\mathbf{q}_2, \mathbf{k}_i, E), \quad (17)$$

where the distortion factors $D^{(\pm)}$ are defined by

$$\begin{aligned} D^{(\pm)}(\mathbf{k}, \mathbf{q}; E) &\equiv \langle \mathbf{k} | \Omega_V^{(\pm)}(E) | \mathbf{q} \rangle \\ &= (2\pi)^3 \delta(\mathbf{k} - \mathbf{q}) + T_V^{(\pm)}(\mathbf{k}, \mathbf{q}; E) \frac{1}{E - E(\mathbf{q}) \pm i\delta}. \end{aligned} \quad (18)$$

The sum over q_1 and q_2 is

$$\sum_{\bar{q}_1, \bar{q}_2} \equiv \int \frac{d\mathbf{q}_1}{(2\pi)^3} \int \frac{d\mathbf{q}_2}{(2\pi)^3},$$

and $E = E(k_f) = E(k_i)$ is the scattering energy. In Eq. (17) we neglected the small contributions, which might come from the single-isobaric analog intermediate states. $T_V^{(\pm)}$ in Eq. (18) are the elastic pion scattering

amplitudes in the initial and final channels. For nuclei such as ^{14}C and ^{18}O , which have the isospin $T_0 = 1$, one may realize that, by ignoring the Coulomb potential, the distortion factors of the initial and final states could be identical and, therefore,

$$D_{\pi^-, \text{DIAS}}^{(\pm)} = D_{\pi^-, \text{g.s.}}^{(\pm)}. \quad (19)$$

D. Partial-wave expansion

Let us decompose all of the quantities in Eq. (17) into the partial-wave series

$$\langle \mathbf{k} | \hat{O}(E) | \mathbf{q} \rangle = 4\pi \sum_{\alpha} \bar{Y}_{\alpha}(\hat{k}) \mathcal{Y}_{\alpha}(\hat{q}) O_{\alpha}(k, q), \quad (20)$$

where α denotes the quantum numbers of a given partial channel, e.g., the orbital angular momentum (l), total angular momentum (I), isospin (T), etc. To simplify the formulation, we consider the case of spinless nuclei having isospin $T_0 = 1$. In this case $\alpha = (l, I)$, where $I = T_0 \pm 1, T_0$. For the partial-wave components of T_2^{DWBA} we obtain

$$\begin{aligned} \mathcal{T}_{2,\alpha}^{\text{DWBA}}(E) &= \int_0^{\infty} \frac{q_1^2 dq_1}{2\pi^2} \int_0^{\infty} \frac{q_2^2 dq_2}{2\pi^2} D_{\alpha}^{(-)+}(k_f, q_1; E) \\ &\quad \times \mathcal{T}_{2,\alpha}^{\text{PWBA}}(q_1, q_2; E) D_{\alpha}^{(+)}(q_2, k_i; E), \end{aligned} \quad (21)$$

where the partial components of the distortion factors are

$$\begin{aligned} D_{\alpha}^{(\pm)}(k, q; E) &= \frac{2\pi^2}{k^2} \delta(k - q) \\ &\quad + T_{\alpha}^{(\pm)}(k, q; E) \frac{1}{E - E(q) \pm i\delta}. \end{aligned} \quad (22)$$

Note that for isoelastic scattering ($k_f = K_i$) there is the identity

$$D_{\alpha}^{(-)+}(k, q; E) = D_{\alpha}^{(+)}(q, k; E). \quad (23)$$

E. On-shell distortion factor

If we neglect the off-energy-shell part of the Green function in Eq. (22), then by combining the on-energy-shell part of Eq. (22) with Eq. (21) and integrating over q_1 and q_2 we get

$$\begin{aligned} \mathcal{T}_{2,\alpha}^{\text{DWBA}}(k_f, k_i; \text{on-shell}) &= \tilde{\gamma}_{\alpha}^{\text{DW}}(k_f, k_i) \mathcal{T}_{2,\alpha}^{\text{PWBA}}(k_f, k_i; E(k)), \end{aligned} \quad (24)$$

where the distortion factor $\tilde{\gamma}(k_f, k_i)$ is defined by

$$\tilde{\gamma}_{\alpha}^{\text{DW}}(k_f, k_i; \text{on-shell}) = [1 + ik_f F_{\alpha}(k_f)][1 + ik_i F_{\alpha}(k_i)]. \quad (25)$$

Here $F_{\alpha}(k)$ is the π -nucleus elastic scattering amplitude given by

$$F_{\alpha}(k) = -\frac{\bar{\omega}}{2\pi} T_{\alpha}^{(+)}(k, k; E(k)), \quad (26)$$

where $\bar{\omega}$ is the reduced pion-nucleus mass.

F. Off-shell distortion factors

The greatest difficulty comes from the problem of taking into account the effects of the off-energy-shell pion distortion, which is related to the principal value integration in Eq. (22). We use an approach based on approximating our optical potential by a separable interaction. Here we use a rank-1 separable potential. Within the framework of this model, the off-shell T matrix is expressed in terms of the on-shell scattering matrix,

$$\mathcal{T}_{\alpha}(q_1, q_2; E) = T_{\alpha}(k, k; E(k)) \frac{g_{\alpha}(q_1) g_{\alpha}(q_2)}{g_{\alpha}^2(k)}. \quad (27)$$

Here, $g(q)$ is the pion-nucleus form factor defined in Sec. III. It is also natural to assume that the identical form factor could be used for the off-shell behavior of the PW amplitude in Eq. (21). Using Eq. (27) we obtain

$$\mathcal{T}_{2,\alpha}^{\text{DWBA}}(k_f, k_i; E) = \gamma_{\alpha}^{\text{DW}}(k_f, k_i) \mathcal{T}_{2,\alpha}^{\text{PWBA}}(k_f, k_i; E), \quad (28)$$

where

$$\gamma_{\alpha}^{\text{DW}}(k_f, k_i) = [1 - k_f F_{\alpha}(k_f) \xi_{\alpha}(k_f)][1 - k_i F_{\alpha}(k_i) \xi_{\alpha}(k_i)] \quad (29)$$

and

$$\xi_{\alpha}(k) = \frac{1}{\pi \epsilon_{\pi A}(k)} \int_0^{\infty} \frac{q^2 dq}{2\pi^2} \left[\frac{g_{\alpha}(q)}{g_{\alpha}(k)} \right]^2 \frac{1}{E(k) - E(q) + i\delta}. \quad (30)$$

Here

$$\epsilon_{\pi A}(k) = k^2 / [2\pi^2 dE(k)/dk] = k\bar{\omega}/2\pi^2$$

is the level density of the scattering states. For isoelastic scattering, $k_i = k_f$. If we neglect the principal value part of the integral in Eq. (30), the distortion factor (29) reduces to the on-shell result given by Eq. (25).

III. PION-NUCLEUS FORM FACTOR

In this section, we outline the procedure of determining the π - A form factor following the Bateman method [23]. The Bateman method consists of approximating a given short-range interaction by a separable potential of rank N ,

$$V_L(k', k) \approx V_L^{(N)}(k', k) = \sum_{i,j=1}^N V_L(k', s_i) (d_L^{-1})_{ij} V_L(s_j, k). \quad (31)$$

Here, $V_L(k', k)$ is the partial-wave component of a given potential $V(\mathbf{k}', \mathbf{k})$,

$$V(\mathbf{k}', \mathbf{k}) = \sum_{L=0}^{\infty} (2L+1) P_L(\hat{\mathbf{k}} \cdot \hat{\mathbf{k}}') V_L(k, k'). \quad (32)$$

The quantities $d_{ij} = V_L(s_i, s_j)$ and s_i specify values of k and k' at which the approximate potential surface $V_L^{(N)}(k', k)$ coincides with the initial surface $V_L(k', k)$.

We assume that at low energies π - A elastic scattering can be represented in terms of $N = 1$, i.e., a separable rank-1 potential. At any given partial wave, the rank-1 potential component is given by

$$V_L(k', k) = V_L^{(1)}(k', k) = \lim_{s \rightarrow 0} \frac{V_L(k', s) V_L(s, k)}{V_L(s, s)}. \quad (33)$$

There are a number of different optical potentials that equally well describe the low-energy π - A interaction [18–21]. It has been shown [19] that all these potentials are closely related to the Kisslinger potential. This globally parametrized potential is given by

$$\frac{-2\bar{\omega}}{4\pi} U(r) = b_{\text{eff}} \rho(r) - c_{\text{eff}} \nabla \cdot \rho(r) \nabla + c_{\text{eff}} \frac{\bar{\omega}}{2M} \nabla^2 \rho(r), \quad (34)$$

where $\bar{\omega}$ is the π - A reduced mass, $\rho(r)$ is the nuclear density, and b_{eff} and c_{eff} are complex, energy-dependent parameters.

The π -nucleus potential (34) in the momentum space is of the form

$$V(\mathbf{k}', \mathbf{k}) \equiv -\frac{2\bar{\omega}}{4\pi} U(\mathbf{k}', \mathbf{k}) = \rho(\mathbf{k}', \mathbf{k}) [a_1 + a_2(k^2 + k'^2) + a_3(\mathbf{k}' \cdot \mathbf{k})], \quad (35)$$

where $a_1 \equiv b_{\text{eff}}$, $a_2 \equiv c_{\text{eff}} \bar{\omega} / 2M$, $a_3 \equiv c_{\text{eff}} (1 - \bar{\omega} / 2M)$, and where

$$\rho(\mathbf{k}', \mathbf{k}) = \int d\mathbf{r} e^{i(\mathbf{k}' - \mathbf{k}) \cdot \mathbf{r}} \rho(r) \quad (36)$$

is the nuclear form factor. Expanding the potential (35) into a partial-wave series, we obtain

$$V_L(k', k) = \rho_L(k', k) [a_1 + a_2(k^2 + k'^2)] + \frac{a_3 k k'}{(2L+1)} [L \rho_{L-1}(k', k) + (L+1) \rho_{L+1}(k', k)], \quad (37)$$

where

$$\rho_L(k', k) = 4\pi \int_0^\infty dr r^2 \rho(r) j_L(k'r) j_L(kr), \quad (38)$$

with $j_L(z)$ a spherical Bessel function.

Equation (35) exhibits a well-known feature of the Kisslinger-type optical potentials; namely, a divergence of the diagonal matrix elements ($\mathbf{k}' = \mathbf{k}$) as $k \rightarrow \infty$. Such a behavior is a consequence of using the zero-range approximation for the p -wave pion-nucleon interaction. This large- k structure complicates the solution of the Klein-Gordon equation in the momentum space, but in practice one can obtain a stable solution by artificially introducing πN form factors and letting a cutoff parameter characterizing its range become large [22]. In our application of the Bateman method, the large- k (small- r) behavior of the optical potential likewise causes no essential problem because the separable approximation of this method expressed in Eq. (31) is applicable to any short-range potential.

In Ref. [22], it was noted that the rate at which the numerical results converge with the cutoff parameter was correlated with the proximity to the so-called Kisslinger singularity. Near this point, cross sections and wave functions are strongly influenced by the far off-shell components of the optical potential. The Kisslinger singularity, which is a property of the lowest-order optical potential at low energy, also causes an enhanced sensitivity of these quantities to the cutoff parameter. It might be argued from this that the Kisslinger potential is inappropriate for applications to low-energy pion-nucleus scattering. However, the sensitivity to the cutoff parameter decreases if higher-order corrections to the optical potential are taken into account properly. For example, the pion-nucleus wave function was studied in coordinate space in Ref. [16], and it was shown here how the anomaly is reduced if one includes the well-known Lorentz-Lorenz–Ericson–Ericson effect and other higher-order terms in the optical potential. These are taken into account in our potential through the values of the effective parameters appearing in Eq. (34). For these reasons, the large-momentum behavior of the optical potential in Eq. (34) should not cause any special problem for our application of the Bateman method.

To apply the Bateman procedure to the partial-wave component (37) of the optical potential, one should factorize a trivial power dependence of momenta $(kk')^L$ out of each partial wave,

$$V_L(k', k) = k'^L k^L \tilde{V}_L(k', k), \quad (39)$$

and approximate $\tilde{V}_L(k', k)$ in Eq. (39) according to Eq. (33),

$$\tilde{V}_L(k', k) \approx \tilde{V}_L^{(1)}(k', k) = \lim_{s \rightarrow 0} \tilde{V}_L(k', s) \tilde{V}_L(s, k) / \tilde{V}_L(s, s). \quad (40)$$

This factorization has made it possible to use the same value, $s = 0$, for all partial waves.

In our calculation we use a Gaussian-type nuclear density,

$$\rho(r) = \rho_0 (1 + w\alpha r^2) \exp(-\alpha r^2), \quad (41)$$

of which the partial-wave component $\rho_L(k', k)$ reads as

$$\begin{aligned} \rho_L(k', k) &= \frac{2\pi^2}{2L+1} \rho_0 \frac{1}{(kk')^{1/2}} D_L(k', k) \\ &\times \left[1 + w \left(1 - \frac{kk'}{2\alpha} \right) \right] \\ &+ w \frac{kk'}{4\alpha} [D_{L-1}(k', k) + D_{L+1}(k', k)]. \end{aligned} \quad (42)$$

Here,

$$D_L(k', k) = \frac{1}{2\alpha} \exp \left[-\frac{k^2 + k'^2}{4\alpha} \right] I_L \left(\frac{kk'}{2\alpha} \right). \quad (43)$$

Taking into account that the modified Bessel function $I_{L+1/2}(z) \sim z^{L+1/2}$ as $z \rightarrow 0$, we identify the momenta $(kk')^L$ in Eq. (39) to be factored from the partial-wave potential $V_L(k'k)$.

Now, using Eq. (40), we obtain the following approximation for the potential in Eq. (35):

$$V_L(k'k) = g_L(k') g_L(k) \gamma_L, \quad (44)$$

where the π -nucleus form factors are of the form

$$g_L(k) = k^L \exp(-z) [1 - \beta_1 z - \beta_2 z^2], \quad z = k^2/4\alpha. \quad (45)$$

The strength parameter is given by

$$\gamma_L = \frac{2\pi}{(2L+1)!!} \frac{1}{(2\alpha)^{L+1}} \left(\frac{\pi}{\alpha} \right)^{1/2} G_L, \quad (46)$$

$$G_L \equiv \rho_0 \left[a_1 \left(1 + w \frac{2L+3}{2} \right) + 2\alpha a_3 L \left(1 + w \frac{2L+1}{2} \right) \right],$$

and the parameters β_1 and β_2 are

$$\beta_1 = \{w(1+L\eta) - 2\epsilon R[1 + w(L + \frac{3}{2})]\} / D_L, \quad (47)$$

$$\beta_2 = 2w\epsilon R / D_L,$$

where

$$D_L = 1 + L\eta + w(L + \frac{3}{2}) \left(1 + \frac{L(2L+1)}{2L+3} \eta \right)$$

and

$$\eta = 2(1 - \epsilon)R.$$

Here $\epsilon = \bar{w}/M$, M is the mass of the nucleon, a_1 , a_2 , and a_3 are the parameters of the optical potential given in Eq. (35), $R = \alpha c_{\text{eff}}/b_{\text{eff}}$, and α and w are the parameters determining the nuclear density.

IV. NUMERICAL CALCULATIONS, RESULTS, AND CONCLUSIONS

In this section, we present the results of the analysis of the distortion effects for the double-isobaric analog transitions for ^{14}C , i.e., the $^{14}\text{C}(\pi^+, \pi^-)^{14}\text{O}(\text{DIAS})$

reaction at pion kinetic energy $T_\pi = 50$ MeV. Specifically, we study the effect of pion external distortions on the sequential mechanism. The isotensor potential U_2^{NAR} [Eq. (4)] is formed from a model of sequential scattering [5] built up from nonanalog excitations of the intermediate nucleus, including the effects of short-range nucleon-nucleon correlations, the intermediate ρ meson, and finite-range meson-nucleon form factors. The full spin dependence of various contributions has been taken into account. For our final results, we will take T_V^{AR} of Eq. (14) from the numerical solution of the Klein-Gordon equation with U_0 and U_1 as described in Secs. II A and III. By virtue of our method of calculation, the internal and external distortions are included in this term. The effects of medium modification corrections to the pion-nucleon scattering amplitude for this contribution will be shown also.

Our calculation of the contribution of nonanalog routes to sequential scattering, included through $U_2 = U_2^{\text{NAR}}$ in Eq. (14), will not be as complete as that of the analog route, due to the absence of internal distortions and the medium modifications to the pion-nucleon interaction in the results of Ref. [5], from which we obtain this contribution. We do not consider this to be a drawback, as it is interesting to understand the separate effects of internal and external distortions on the DCX amplitude in Eq. (14). Internal distortions involve a somewhat different set of issues and require a separate theoretical study. A comparison, including internal as well as external distortions, to all the data that exists for DIAS transitions with a ^{14}C target will be presented in a subsequent publication.

A. Distortion factors

According to Eqs. (25) and (29), we write the distortion factors as a sum of two terms,

$$\begin{aligned} \gamma_\alpha^{\text{DW}}(k_f, k_i) &= \gamma_\alpha^{\text{DW}}(k_f, k_i; \text{on-shell}) \\ &+ \gamma_\alpha^{\text{DW}}(k_f, k_i; \text{off-shell}), \end{aligned} \quad (48)$$

where the on-shell distortion factor is expressed in terms of the elastic scattering amplitudes by Eq. (25). The off-shell distortion factor, which is determined by the principal value part of the integral in Eq. (30), depends, in addition, on the pion-nucleus form factors.

To analyze the effect of distortions, it is convenient to represent the distortion factors as

$$\gamma_\alpha^{\text{DW}} = |\gamma_\alpha^{\text{DW}}| e^{i\phi_\alpha}. \quad (49)$$

In Table I we present numerical results demonstrating the contribution of the on- and off-energy-shell distortion factors to the overall distortion effect.

The pion-nucleus scattering amplitudes are calculated using the PIESDEX code, which is described in Ref. [16]. The parameters of the pion-nucleus optical potential [16] and the parameters of the nuclear density [Eq. (41) for ^{14}C] are also taken from Ref. [16].

The pion-nucleus form factors are calculated for the

TABLE I. Contribution of the on- and off-energy-shell distortion factors to the external pion-distortion effect for individual partial waves. The meaning of the definitions is given in Sec. IV A.

L	On-shell		Off-shell		Full	
	$ \gamma_\alpha^{\text{DW}} $	ϕ_α (deg)	$ \gamma_\alpha^{\text{DW}} $	ϕ_α (deg)	$ \gamma_\alpha^{\text{DW}} $	ϕ_α (deg)
0	0.694	-23.33	0.187	-61.28	0.849	-31.11
1	0.727	23.07	0.575	60.08	1.236	39.32
2	0.908	14.21	0.951	34.98	1.829	24.84
3	0.992	2.50	0.549	12.91	1.535	6.20
4	0.999	0.26	0.266	6.25	1.264	1.52
5	1.000	0.02	0.134	3.84	1.134	0.47
6	1.000	0.001	0.071	-3.50	1.071	-0.23

optical potential given in Eq. (34), the parameters of which are taken to be

$$b_{\text{eff}} \text{ (fm)} = -0.074 + i0.018, \quad (50)$$

$$c_{\text{eff}} \text{ (fm}^3\text{)} = 0.427 + i0.040.$$

These values correspond to set E of the Michigan State University (MSU) optical potential [18]; of the various sets considered in this paper, this one provides the best fit to the 50 MeV elastic scattering data.

The π -nucleus form factors in Eq. (45) are complex due to the fact that optical potential parameters Eq. (34) are complex themselves. However, in our calculations, we neglected the imaginary parts of the parameters b_{eff} and c_{eff} , i.e., we use for R in Eq. (47)

$$R = \alpha \frac{\text{Re}c_{\text{eff}}}{\text{Re}b_{\text{eff}}}. \quad (51)$$

We have estimated the imaginary parts of the parameters $\beta_{1,2}$ and found that these parts are negligible in the low-energy region.

It is seen from Table I that the external distortion strongly influences the angular distribution. The absolute value of the distortion factors [see Eq. (49)] $|\gamma_\alpha^{\text{DW}}|$ reaches the value ~ 2 for the D wave, then decreasing to unity with increasing orbital angular momentum. The phases ϕ_α of the distortion factors also strongly change the plane-wave results, especially for S and P waves. The results presented in Table I also show that both the on- and off-shell distortions are important, although the major contribution comes from the on-shell piece.

B. Distortion effect for SEQ

Before applying our results using Eq. (14), we consider the effect of the external distortions to U_2^{SEQ} [see the discussion in connection with Eq. (4)]. In Fig. 1 we present results of our calculations of the differential cross section for DCX to DIAS for ^{14}C using this amplitude. The PW result is given by the dashed line. The on-shell external distortion (short-dashed line) decreases the PW angular distribution substantially over the entire range of scattering angles. Turning on the off-shell distortion (solid line) changes the PW result qualitatively, increasing it at

forward angles and decreasing it at large angles.

The same qualitative effect of the external distortion seen in Fig. 1 has been obtained in [8] using the DWIA. We take this as a confirmation of our approximation scheme, concluding that one of our objectives has been accomplished, namely, to develop a method for including external distortions that is equivalent to the DWIA, but simpler. Having confirmed our approximation, we turn next to making a more complete theory.

C. Analog-route transition

The results based on the second Born approximation using closure, such as those shown in Fig. 1, are incomplete for several reasons that have been discussed earlier. One is that the pion wave, internal to U_2^{SEQ} , has been

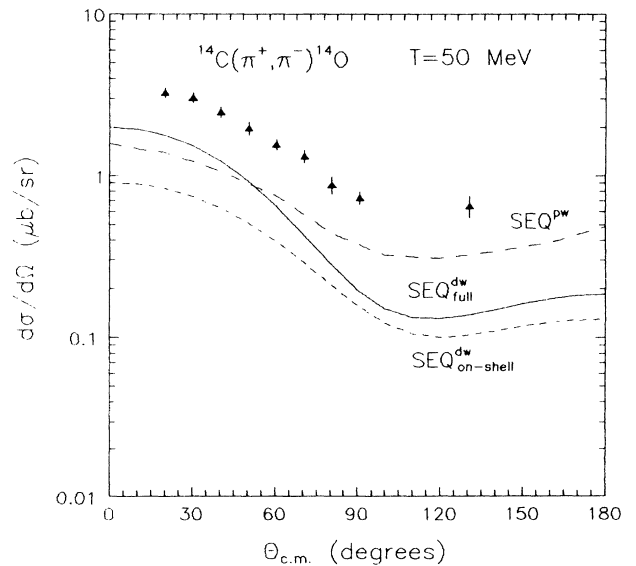


FIG. 1. Differential cross sections for DCX $^{14}\text{C}(\pi^+, \pi^-)^{14}\text{O}$ to the DIAS at $T_\pi = 50$ MeV. Calculations have been done for the sequential mechanism. The dashed line corresponds to the PW results [5], the solid line is for the full result, and the short-dashed line is for just on-shell external pion distortions. The experimental data are taken from Ref. [4].

taken as a plane wave in Ref. [5]. Another one, motivating us to introduce the isospin invariant model in Sec. II, is that the AR contribution implicit in U_2^{SEQ} is not realistic; this will be remedied below following the discussion in Sec. II A and II B.

The analog-route transitions within the framework of the isospin-invariant optical model (Sec. II A) are calculated by solving the Klein-Gordon equation with the isoscalar (U_0) and isovector (U_1) potentials. For numerical calculations we use PIESDEX [16] code. In our model U_0 and U_1 contain not only a lowest-order piece built up in the standard way from the free pion-nucleon scattering amplitude, but also a second-order piece including short-range and Pauli correlations. In any meaningful discussion of DCX, it is crucial to confirm that the cross sections of elastic and SCX to isobaric analog states are well reproduced by these ingredients from which the analog route are constructed.

Consider first SCX scattering to the IAS within the framework of the isospin-invariant optical model. In Fig. 2 we show the results of the description of SCX to the IAS for $^{14}\text{C}(\pi^+, \pi^0)^{14}\text{N}(E^* = 2.3 \text{ MeV})(\text{IAS})$ at 50 MeV. The solid curve in this figure represents the full calculation in which the isovector potential U_1 includes both the isovector correlation term (ELIV, Lorentz-Lorentz isovector) and an imaginary second-order p -wave isovector term [$\lambda_{p1}^{(2)} = (0 - i1.0) \text{ fm}^{-3}$]. The last term was introduced phenomenologically in Ref. [5] to provide the best fit to the data, and we use this potential in our calculations of the AR amplitude for DCX to the DIAS, i.e., T_V^{AR} .

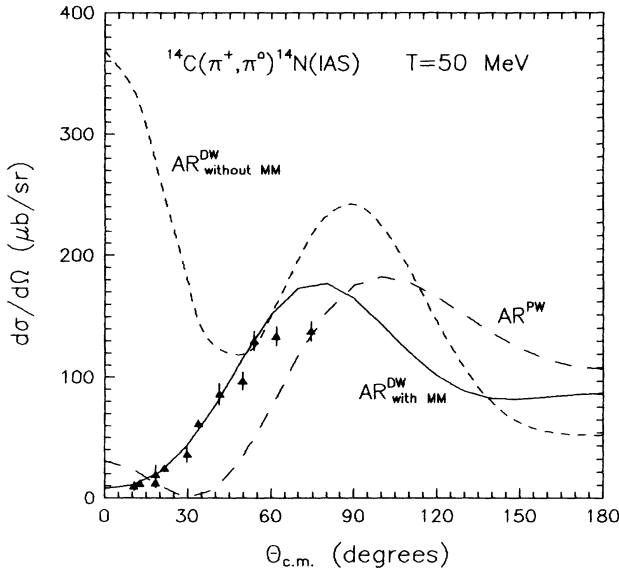


FIG. 2. Calculations of $^{14}\text{C}(\pi^+, \pi^0)^{14}\text{N}$ to the IAS at $T_\pi = 50 \text{ MeV}$. The solid curve shows the result of the full calculation, including medium modification (MM) effects [via the isovector correlation ELIV term and an imaginary second-order p -wave isovector term $\lambda_{(p1)}^2 = (0 - i1.0) \text{ fm}^{-3}$]. The short-dashed curve is obtained when the MM corrections are turned off. The long-dashed curve is obtained in the PW approximation. The experimental data are from Ref. [25].

In Fig. 2, we also present the differential SCX cross sections calculated with the lowest-order isovector optical potential when the medium modification corrections are turned on (solid curve) and turned off (short-dashed curve), and in the PW approximation for the lowest-order isovector potential (long-dashed curve). These calculations show the role of external pion distortions and the medium modification corrections.

The difference between the long-dashed and the short-dashed curve shows the effect of the pion distortion on SCX to the IAS, and the difference between the solid and the short-dashed one shows the effect of the medium corrections. The most dramatic effect, as noted in [5], can be seen in the forward direction, where the ELIV term changes the maximum at $\theta = 0^\circ$ into a minimum. This is clearly a strong medium modification effect. One can also conclude, comparing the solid curve with the long-dashed curve (the PW approximation), that the medium modification corrections tend to cancel the effect of the pion distortion.

Consider next the contribution of the AR to DCX. The calculation of it in second order using the lowest-order isovector optical potential [see Eq. (A5) in the Appendix] gives

$$\mathcal{T}_2(\text{AR}) = \langle \psi_{\mathbf{k}_f}^{(-)}(\pi^-; \text{DIAS}) | \Delta U_2^{\text{AR}} | \psi_{\mathbf{k}_i}^{(+)}(\pi^+; \text{g.s.}) \rangle .$$

The result, which is obtained following a procedure similar to that used for the analog-route contribution of U_2^{SEQ} , is shown in Fig. 3. The dashed line shows the PW approximation. The on-shell external distortions (short-dashed line) decrease the PW angular distribution substantially over the entire range of scattering angles. Turning on the off-shell distortion (solid line) changes the PW result qualitatively, increasing it at both small

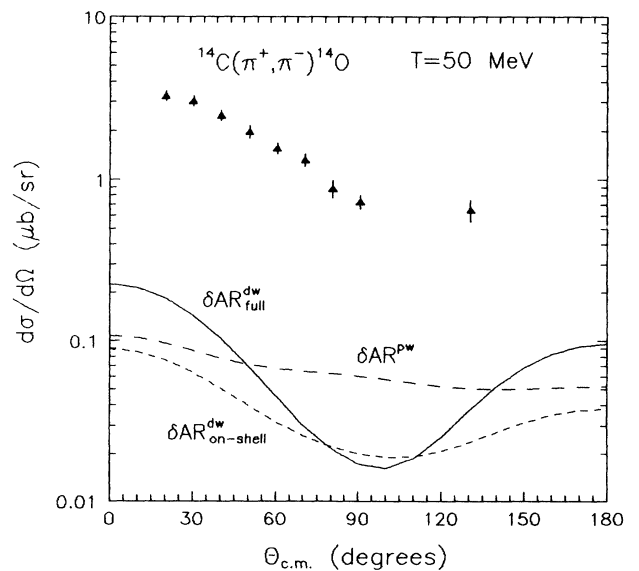


FIG. 3. Contribution of the analog route to the differential cross sections of Fig. 1. The meaning of the curves is the same as in Fig. 1.

and large angles, and decreasing at angles around 90° .

In Fig. 4 we compare the AR with external distortions (short-dashed line) taken from Fig. 3 with the corresponding AR calculation (dashed curve) taken from Ref. [16] (calculated with the lowest-order optical potential $U_1^{(1)}$). This result includes the internal as well as external distortions of the pion, as it results from a full optical potential calculation. We see that the internal distortions, at least for the AR piece of the amplitude, change the cross section drastically, increasing it by an order of magnitude at forward angles.

The lowest-order optical potential does not contain the isovector correlation term (ELIV), which strongly affects the SCX (see Fig. 2) and DCX cross sections, as has been demonstrated in Ref. [16] (see Figs. 3 and 4 therein). The solid curve in Fig. 4 shows the result of the optical model calculation including the full U_1 (including the isovector ELIV term and the second-order isovector absorption-dispersion term of Ref. [16], needed to improve the small-angle SCX cross section). We see by comparing the dashed and solid curves that the second-order isovector effects are very important corrections for the AR.

D. Nonanalog route transition

In Fig. 5, we show the effect of external distortions on U_2^{NAR} . The PW result is given by the dashed line. The on-shell distortions (short-dashed line) decrease the PW angular distribution substantially over the entire range of scattering angles. Turning on the off-shell distortion

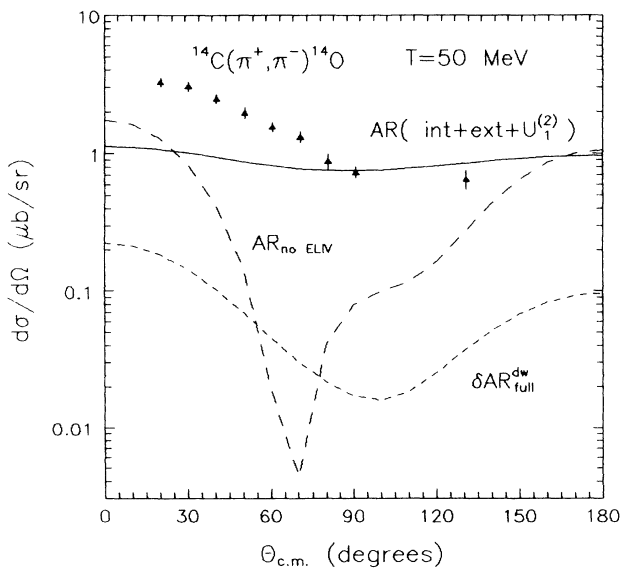


FIG. 4. DCX differential cross sections for the analog route $^{14}\text{C}(\pi^+, \pi^-)^{14}\text{O}$ to the DIAS at 50 MeV. The solid curve represents the AR transitions calculated from the PIESDEX code [16] with the $U_1^{(2)}$ contribution; the dashed curve is the same but without the ELIV term of isovector potential; the short-dashed curve corresponds to the solid curve of Fig. 3.

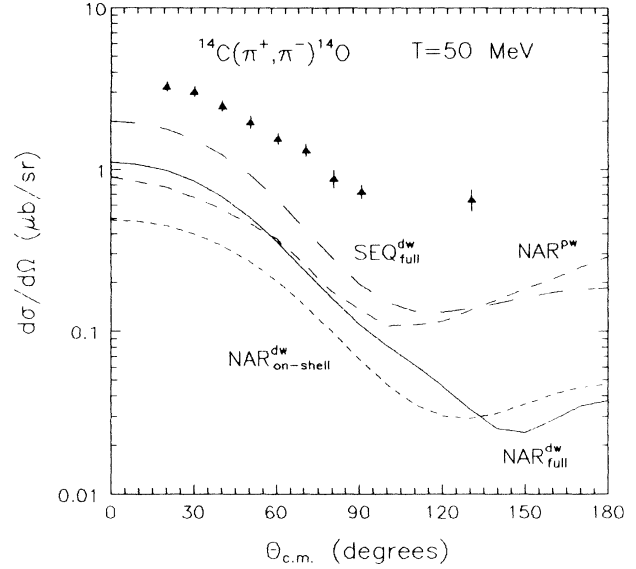


FIG. 5. Contribution of the nonanalog route to the differential cross sections of Fig. 1. The meaning of the curves is the same as in Fig. 1. The sequential mechanism with external distortions, given by the long-dashed curve, is also reproduced.

(solid line) changes the PW result qualitatively, increasing it at forward angles and decreasing it at large angles. The results are qualitatively, but of course not quantitatively, similar to the results obtained for cases shown in Fig. 1. The difference between the solid line and the long-dashed line (the SEQ with external distortions, taken from Fig. 1) shows the AR contribution to the SEQ amplitude.

As we said earlier, these results may be changed when the internal distortions of the pion are considered in U_2^{NAR} . Some guidance for what to expect may be obtained from examining Fig. 2, where it is seen that, while distortions alone have a major effect on the SCX cross section, once the medium modifications are included, the result comes back close to the original PW result. It will be interesting to see the extent to which the tendency for the internal distortions to cancel the medium modifications persists for U_2^{NAR} . For now, we will proceed under the assumption that the cancellation is exact for this term.

E. Combined results

In Fig. 6, we show the analog-route contribution as the short-dashed curve (as in Fig. 4) and the nonanalog-route contribution as the dashed line (as in Fig. 5). The combined amplitude of Eq. (14) is shown as the solid line. We note that the combined result is comparable to the experimental data throughout the entire angular range.

From Fig. 6 it is seen that, though the AR contribution to the SEQ- π amplitude is moderately small, this am-

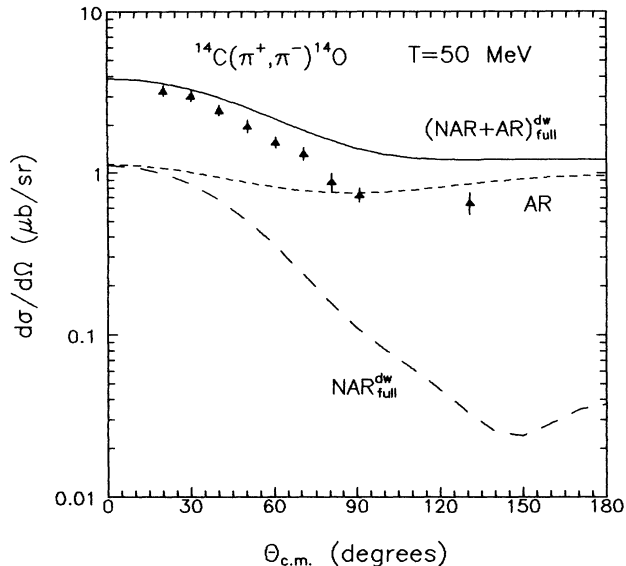


FIG. 6. Differential cross sections for DCX $^{14}\text{C}(\pi^+, \pi^-)^{14}\text{O}$ to the DIAS at 50 MeV. The dashed curve represents the DW NAR contribution; the short-dashed curve corresponds to the solid curve of Fig. 4; the solid curve is a summary of the NAR and AR mechanisms given above.

plitude interferes constructively with the isotensor NAR amplitude, giving a larger result than that obtained from U^{SEQ} . It is not surprising that the AR amplitude interferes constructively with the NAR SEQ- π amplitude, which can be understood by comparing the lowest-order AR amplitude ΔF^{AR} determined by Eq. (A6) (see the Appendix) with the NAR SEQ- π amplitude (see Ref. [5]). The relative phase between these two amplitudes is determined mainly by the pion propagators, which are identical and determined by the same Hamiltonian [see Eq. (14) in Sec. II B]. This is especially easy to see if the NAR SEQ- π amplitude is calculated using the closure approximation [5].

We present the combined results for the excitation function over the energy range from 20 to 80 MeV in Fig. 7. We dash the line between 20 and 30 MeV to indicate that Coulomb effects, Q -value effects, and possibly corrections to the closure approximation that we have used for the NAR part of the calculation might play a role at these energies. The excitation function in this energy region is compared to the PW approximation [5], shown by the dashed curve in Fig. 7. In Fig. 8 we show the angular distributions at 30 MeV and above. From Figs. 7 and 8, one can see that the results (except at very low energies) are comparable to the data, just as at 50 MeV (Fig. 6).

Taking into account that the medium modifications (in particular the isovector LLEE, Lorentz-Lorentz-Ericson-Ericson) tend to cancel the distortions (see Fig. 2 for SCX), we expect that our results are realistic and see that the standard sequential mechanism is able to explain the DIAS double-charge-exchange scattering data. However, it is premature to conclude from this that exotic mecha-

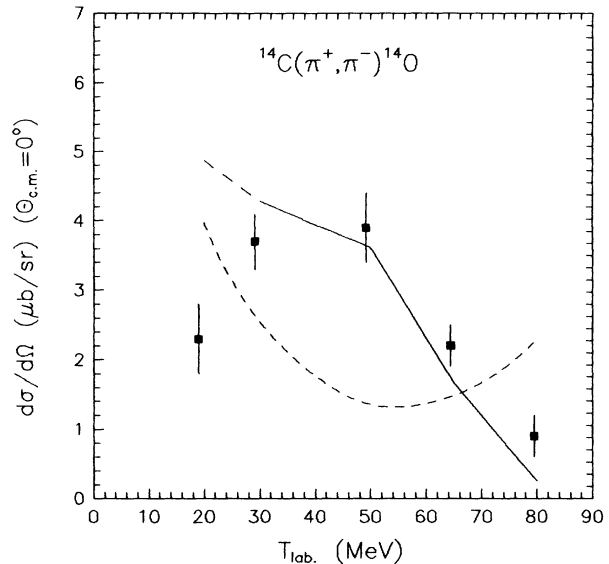


FIG. 7. Energy dependence of $\theta = 0^\circ$ DCX cross section. The dashed curve is the PW result for the standard (SEQ- π) model. The solid curve shows the result of the full calculation when both the external DW NAR contribution and AR transitions are taken into account.

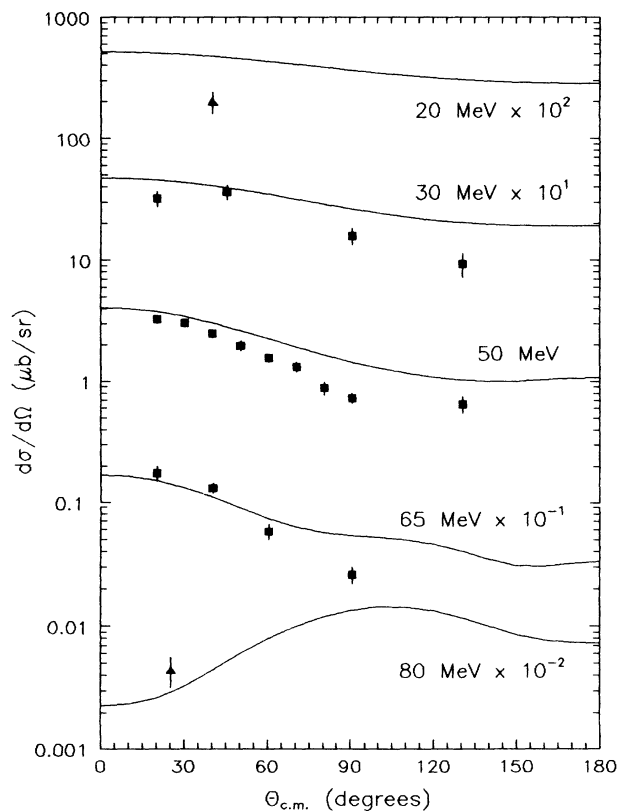


FIG. 8. Differential cross sections for DCX $^{14}\text{C}(\pi^+, \pi^-)^{14}\text{O}$ to the DIAS at different energies. The meaning of the solid curves is the same as in Fig. 6. The experimental data are taken from Ref. [4].

nisms, such as those discussed in the Introduction, do not contribute to low-energy DCX. Before such a conclusion can be drawn, it is necessary to include medium modification and internal distortions in U_2^{NAR} in a consistent way.

F. Conclusion

In this paper, we proposed a simple but effective method of taking into account the external distortion effects based on a separable approximation to our optical potential. We studied the role of external distortions in the particular case of pion-nucleus DCX to the DIAS at low energies. It should be stressed that this method can also be applied to study the effects of external pion distortions in various other reactions, such as photopion absorption and production reactions, pion absorption processes, etc., in which a pion appears in the initial or final state. According to our method, the DW amplitude for such a process is given as the product of the corresponding PW amplitude and a distortion factor, which is expressed in terms of separable pion-nucleus form factors.

As our first application of this method, we studied the external distortion effect on a particular sequential DCX mechanism in which all intermediate states are summed using closure [5]. By comparing to an earlier DWIA study [9] using similar approximations, we have been able to confirm our approximation: we found that the resulting external distortion for the reaction on ^{14}C at 50 MeV strongly modifies the PW results, increasing the angular distribution at forward angles and decreasing it at large angles. We have shown explicitly here that both on- and off-shell distortions are important.

Next, we isolated the contribution of the analog route for DCX to the DIAS for ^{14}C at 50 MeV using the framework of the isospin-invariant optical model. The isoscalar and isovector parts of the optical potential, which drive the AR contribution, have been fitted to the SCX data (see Fig. 2). It was shown that, although the AR contribution to the SEQ- π amplitude is moderately small (see Figs. 6 and 7), this amplitude interferes constructively with the isotensor NAR amplitude, giving a larger result than that obtained from U^{SEQ} .

We also studied the effect of the internal distortion on the AR transitions and showed that this effect strongly changes the cross section calculated in the distorted-wave approximation with only the external distortions taken into account (see Fig. 4). This result indicates the importance of conducting a separate study of the effect of distortions on the virtual pion in the NAR part of the SEQ- π mechanism.

In a recent paper [24] by several of us, a method for calculating the medium modification of pion propagation between two nucleons in finite nuclei was developed. We are presently using this work to determine the size of the internal distortions for double charge exchange, and the findings will be reported in a subsequent publication. Preliminary results indicate a net sequential DCX amplitude, including realistic internal distortions, about 30% larger than the solid curve in Fig. 6. Since these results

do not yet contain the LLIV effect, we anticipate a relatively small correction to the results presented in this paper.

ACKNOWLEDGMENTS

The work is supported in part by the Russian Science Foundation (Project No. 93-02-3833) and U.S. Department of Energy. M.Kh. would like to express his thanks for the hospitality extended by Los Alamos National Laboratory, where the work was started. We would all like to acknowledge the hospitality and support of the Institute for Nuclear Theory of the University of Washington in Seattle, which enable us to continue this work. Two of us (M.B.J. and H.S.) would like to express our appreciation for the hospitality extended by the Joint Institute for Nuclear Research in Dubna where the work was completed. We are also grateful to V. B. Belyaev for discussions.

APPENDIX

In this paper, we have adopted the PW sequential DCX amplitude $T^{\text{SEQ}} \equiv U_2^{\text{SEQ}}$ described in Fig. 1(a) of Ref. [5] as the basis of the isotensor interaction (short-range repulsive correlations acting between the two nucleons are implicit in the figure). This amplitude entails a sum over all intermediate nuclear states, including a piece of T^{AR} [our Eq. (14)], as taken from Ref. [16]. In order to avoid double counting, we must remove the intermediate analog-state contribution

$$\Delta U_2^{\text{AR}} = U_1^{(1)} \hat{P} G(E) U_1^{(1)}, \quad (\text{A1})$$

where $U_1^{(1)}$ is the isovector part of the lowest-order optical potential (1) corresponding to the pion-nucleon scattering amplitude employed in Ref. [5]. Therefore the DCX scattering amplitude is determined now by Eq. (14), where Eq. (15) is replaced by

$$\mathcal{T}_2^{\text{DWBA}} = \langle \psi_{\mathbf{k}_f}^{(-)}(\pi^-; \text{DIAS}) | U_2^{\text{NAR}} | \psi_{\mathbf{k}_i}^{(+)}(\pi^+; \text{g.s.}) \rangle, \quad (\text{A2})$$

and where the isotensor potential U_2^{NAR} is given by

$$U_2^{\text{NAR}} \equiv U_2^{\text{SEQ}} - \Delta U_2^{\text{AR}}. \quad (\text{A3})$$

The analog-route contribution T^{AR} in Eq. (14) is calculated with the lowest-order isovector optical potential following Ref. [16].

In this appendix we describe our procedure of calculating the analog-route contribution to U_2^{SEQ} , which, in terms of the scattering amplitude, reads as

$$\Delta F^{\text{AR}} \equiv -\frac{\bar{\omega}}{2\pi} \Delta U_2^{\text{AR}}, \quad (\text{A4})$$

where $\bar{\omega}$ is the reduced mass of the pion-nucleus system.

To be consistent with the calculation of T^{AR} , we take the lowest-order optical potential in the following form

[compare with Eq. (34)]:

$$-\frac{2\bar{\omega}}{4\pi}U(r) = b_{\text{eff}}^{(1)}\rho(r) - c_{\text{eff}}^{(1)}\nabla \cdot \rho(r)\nabla + c_{\text{eff}}^{(1)}\frac{\bar{\omega}}{2M}\nabla^2\rho(r), \quad (\text{A5})$$

where the parameters $b_{\text{eff}}^{(1)}$ and $c_{\text{eff}}^{(1)}$ are determined (see Ref. [16]) as

$$b_{\text{eff}}^{(1)} \equiv k^2\lambda_{s1}^{(1)}/4\pi A$$

and

$$c_{\text{eff}}^{(1)} \equiv \lambda_{p1}^{(1)}/4\pi A.$$

The parameters $\lambda_{s1}^{(1)}$ and $\lambda_{p1}^{(1)}$ are related to the single-nucleon parameters b_1 and c_1 of the MSU optical potential [8] as

$$b_1 = \lambda_{s1}^{(1)}(k^2/8\pi p_1)$$

and

$$c_1 = \lambda_{p1}^{(1)}(p_1/8\pi),$$

where $p_1 = (1 + \epsilon)/(1 + \epsilon/A)$, $\epsilon = \omega_\pi/M_N$, ω_π is the pion energy, and M_N is the nucleon mass. In the PW approximation the expression for ΔF^{AR} is

$$\begin{aligned} \langle \mathbf{k}_f | \Delta F^{\text{AR}}(PW) | \mathbf{k}_i \rangle &= -\frac{\bar{\omega}}{2\pi} \int \frac{d\mathbf{q}}{(2\pi)^3} \langle \mathbf{k}_f | U_1^{(1)} | \mathbf{q} \rangle \\ &\times \frac{1}{E(k) - E(q) \pm i\delta} \\ &\times \langle \mathbf{k}_f | U_1^{(1)} | \mathbf{k}_i \rangle. \quad (\text{A6}) \end{aligned}$$

Decomposing ΔF^{AR} into the partial-wave series [see Eq. (20)] and using the rank-1 separable approximation to the optical potential (A5) [see Eq. (44)] for a partial-wave component we obtain

$$\begin{aligned} \Delta F_\alpha^{\text{AR}}(\text{PW}) &= -\left(\frac{\bar{\omega}}{2\pi}\right)^2 k U_{1;\alpha}^{(1)}(k_f, k_f) \\ &\times U_{1;\alpha}^{(1)}(k_i, k_i) \xi_\alpha^{(1)}(k_f, k_i), \quad (\text{A7}) \end{aligned}$$

where

$$\begin{aligned} \xi_\alpha^{(1)}(k_f, k_i) &= \frac{1}{\pi \epsilon_{\pi A}(k)} \int_0^\infty \frac{q^2 dq}{2\pi^2} \frac{g_\alpha^2(q)}{g_\alpha(k_f)g_\alpha(k_i)} \\ &\times \frac{1}{E(k_i) - E(q) + i\delta}. \quad (\text{A8}) \end{aligned}$$

The partial-wave components $U_{1;\alpha}^{(1)}$ of the optical potential (A1) and the corresponding pion-nucleus form factors $g_\alpha(k)$ are determined by Eqs. (37) and (45), where the parameters α_i are related to the parameters $b_{\text{eff}}^{(1)}$ and $c_{\text{eff}}^{(1)}$ as $\alpha_1 = b_{\text{eff}}^{(1)}$, $\alpha_2 = c_{\text{eff}}^{(1)}(\bar{\omega}/2M)$, and $\alpha_3 = c_{\text{eff}}^{(1)}(1 - \bar{\omega}/2M)$.

To calculate the effect of the external distortion of the pion wave, we use the same procedure as for U_2^{SEQ} (see Secs. II C–II F). Using Eq. (28) we obtain

$$\Delta F_\alpha^{\text{AR}}(k_f, k_i; \text{DW}) = \gamma_\alpha^{\text{DW}}(k_f, k_i) \Delta F_\alpha^{\text{AR}}(k_f, k_i; \text{PW}), \quad (\text{A9})$$

where the distortion factors $\gamma_\alpha^{\text{DW}}$ are determined in Eq. (29).

-
- [1] J. Navon *et al.*, Phys. Rev. Lett. **52**, 105 (1984).
[2] A. Altman *et al.*, Phys. Rev. Lett. **55**, 1273 (1985).
[3] M. J. Leitch *et al.*, Phys. Rev. Lett. **54**, 14824 (1984).
[4] M. J. Leitch *et al.*, Phys. Rev. C **39**, 2356 (1989).
[5] E. R. Siciliano, M. B. Johnson, and H. Sarafian, Ann. Phys. (N.Y.) **203**, 1 (1990).
[6] T. Karapiperis and M. Kobayashi, Phys. Rev. Lett. **54**, 1230 (1985).
[7] M. Bleszynsky and G. J. Glauber, Phys. Rev. C **36**, 681 (1987).
[8] Q. Haider and L. C. Liu, Z. Phys. A **335**, 437 (1990).
[9] Q. Haider and L. C. Liu, J. Phys. G **14**, 1527 (1988); **15**, 934 (1989).
[10] D. S. Koltun and M. S. Singham, Phys. Rev. C **41**, 2266 (1990).
[11] E. Oset, M. Kh. Khankhasayev, J. Nieves, H. Sarafian, and M. J. Vicente-Vacas, Phys. Rev. C **46**, 2406 (1992).
[12] M. B. Johnson, E. Oset, H. Sarafian, E. R. Siciliano, and M. J. Vicente-Vacas, Phys. Rev. C **44**, 2480 (1991).
[13] M. F. Jiang and D. S. Koltun, Phys. Rev. C **42**, 2662 (1990).
[14] M. B. Johnson, Phys. Rev. C **22**, 192 (1980).
[15] M. B. Johnson and E. R. Siciliano, Phys. Rev. C **27**, 730 (1983).
[16] E. R. Siciliano, M. D. Cooper, M. J. Johnson, and M. J. Leitch, Phys. Rev. C **34**, 267 (1986).
[17] M. L. Goldberger and K. M. Watson, *Collision Theory* (Wiley, New York, 1964), Chap. 5, §4.
[18] K. Stricker, H. McManus, and J. A. Carr, Phys. Rev. C **19**, 929 (1979); **22**, 2043 (1980); J. A. Carr, H. McManus, and K. Stricker, *ibid.* **25**, 952 (1982).
[19] R. Seki, K. Masutani, M. Oka, and K. Yazaki, Phys. Lett. **97B**, 200 (1980); R. Seki and K. Masutani, Phys. Rev. C **27**, 2799 (1983); R. Seki, K. Masutani, and K. Yazaki, *ibid.* **27**, 2817 (1983).
[20] O. Meirav, E. Friedman, A. Altman, M. Mannach, R. R. Johnson, and D. R. Gill, Phys. Lett. B **199**, 5 (1987).
[21] M. Kh. Khankhasayev and N. S. Topilskaya, Phys. Lett. B **217**, 14 (1989).
[22] M. B. Johnson and D. J. Ernst, Phys. Rev. C **20**, 1064 (1979).
[23] V. B. Belyaev, *Lectures on the Theory of Few-Body Systems*, Springer Series in Nuclear and Particle Physics (Springer-Verlag, Berlin, 1990).
[24] H. Sarafian, M. B. Johnson, and E. R. Siciliano, Phys. Rev. C **48**, 1988 (1993).
[25] J. L. Ullmann *et al.*, Phys. Rev. C **33**, 2092 (1986).